Tikrit Journal of Engineering Sciences (2024); 31(1): 262-277
DOI: http://doi.org/10.25130/tjes.31.1.22

IRAQI Academic Scientific Journals

ISSN: 1813-162X (Print); 2312-7589 (Online)
Tikrit Journal of Engineering Sciences
available online at: http://www.tj-es.com

TJES Tikrit Journal of Engineering Sciences

Experimental Investigation of CO_2 Solubility in New Amine-Based Deep Eutectic Solvents

Mohammed N. Jassim [a*], Thamer J. Mohammed [a], Abdul Mun'em Abbas Karim [b]

a Department of Chemical Engineering, Engineering College, University of Technology, Baghdad, Iraq.
b Department of Chemical Engineering, College of Engineering, Diyala University, Diyala, Iraq.

Keywords:
CO2 Absorption; Deep Eutectic; Energy; Environment; Greenhouse.

Highlights:

- The research aims to find the most suitable solvent for CO2 capture in synthetic gas mixtures, comparing deep eutectic and standard solvents.
- It also examines the impact of factors like solvent temperature, concentration, and absorption duration on carbon dioxide capture.
- The ultimate goal is to improve the performance of the chosen solvent, determine optimal CO2 capture working conditions, and calculate the reaction rate constant and reaction order for the chosen solvent.

ARTICLE INFO
Article history:

Received	19 June	2023
Received in revised form	21 July	2023
Accepted	21 Sep.	2023
Final Proofreading	26 Nov.	2023
Available online	15 Mar.	2024

Citation: Jassim MN, Mohammed TJ, Karim AA. **Experimental Investigation of CO2 Solubility in New Amine-Based Deep Eutectic Solvents**. *Tikrit Journal of Engineering Sciences* 2024; **31**(1): 262-277. http://doi.org/10.25130/tjes.31.1.22

*Corresponding author:
Mohammed N. Jassim
Department of Chemical Engineering, Engineering College, University of Technology, Baghdad, Iraq.

Abstract: The growing concern about global warming and climate has raised the research field dedicated to finding solutions. One area that has received considerable attention is the exponential increase of carbon dioxide emissions from the atmosphere from the petroleum and gas industries. So, to solve this problem, researchers investigated new ways to collect CO_2 from the air depending on the fact that CO_2 is soluble in water because using aqueous amine absorbents to collect CO_2 has a lot of drawbacks, such as the need for tremendous energy to recycle the solvent and high operational costs. In this study, a specific type of deep eutectic solvent (DES), namely Choline chloride + monoethanolamine (ChCl-MEA), was used as a promising solvent in the CO_2 capture process. Solubility measurements were conducted at 1:6 molar ratios. The amines chosen are typical of basic amines. Experiment absorption data were investigated at various parameters, including a concentration range of 0–3 mol/L, temperatures ranging from 25 to 45 °C, and absorption durations ranging from 60 to 120 minutes, to get the best conditions for high-loading CO_2 uptake. The study found that amine-based DESs had a significantly greater absorption capacity than monoethanolamine-based and conventional DESs. The study examined what happened when water was added to a deep eutectic solvent made of choline chloride and monoethanolamine (ChCl-MEA DES). The most effective way to absorb CO_2 was physical absorption, which can hold 276.13 mol CO_2 per gram of DES at 1 bar and 29.025 °C when mixed with water. The deep eutectic was mixed with water to increase the absorption efficiency. 10 ml of aqueous solution (DESs + water) was taken. The combination of DES and water significantly increased CO_2's low solubility. The modified Design-Expert model satisfactorily represents the experimental solubility of CO_2 in the solvent. The average percent differences between experimental and projected values were 10.7% and 6.8% for binary and ternary systems, respectively. The optimal conditions for maximum absorption rate were 29.025°C, 2.233 mol/L, and 101 minutes, with an absorption ratio of 0.0734 mol/kg.min and efficiency of absorption of 85.3% for solution DESs and water.

دراسة تجريبية لقابلية ذوبان ثاني أكسيد الكربون في المذيبات العميقة سهلة الانصهار القائمة على الأمينات

محمد نوري جاسم[1]، ثامر جاسم محمد[1]، عبد المنعم عباس كريم[2]

[1] قسم الهندسة الكيمياوية / كلية الهندسة / الجامعة التكنولوجية / بغداد – العراق.

[2] قسم الهندسة الكيمياوية / كلية الهندسة / جامعة ديالى / ديالى – العراق.

الخلاصة

قد أدى القلق المتزايد بشأن ظاهرة الاحتباس الحراري وتغير المناخ بدوره إلى ظهور مجال بحثي مخصص لإيجاد الحلول. أحد المجالات المحددة التي حظيت باهتمام كبير هو الزيادة الهائلة في انبعاثات ثاني أكسيد الكربون في الغلاف الجوي من صناعات النفط والغاز. لذا، لحل هذه المشكلة، بحث الباحثون في طرق جديدة لجمع ثاني أكسيد الكربون من الهواء باستخدام حقيقة أن ثاني أكسيد الكربون قابل للذوبان في الماء. وذلك لأن استخدام ماصات الأمينات المائية لتجميع ثاني أكسيد الكربون له الكثير من العيوب، مثل الحاجة إلى الكثير من الطاقة لإعادة تدوير المذيب وارتفاع تكاليف التشغيل. في هذه الدراسة، تم استخدام نوع محدد من المذيبات العميقة سهلة الانصهار (DES) ، وهي كلوريد الكولو + أحادي إيثانول أمين (ChCl-MEA)، كمذيب واعد في عملية احتجاز ثاني أكسيد الكربون. أجريت قياسات الذوبان بنسب مولية ١:٦. الأمينات المختارة نموذجية للأمينات الأساسية. تم إجراء بيانات امتصاص التجربة بمعلمات مختلفة، بما في ذلك نطاق تركيز من ٠ إلى ٣ مول/لتر، ودرجات حرارة تتراوح من ٢٥ إلى ٤٥ درجة مئوية، وفترات امتصاص تتراوح من ٦٠ إلى ١٢٠ دقيقة، للحصول على أفضل الظروف للتحميل العالي. امتصاص ثاني أكسيد الكربون. وجدت الدراسة أن DESs المستندة إلى الأمينات لديها قدرة امتصاص أكبر بكثير من DESs القائمة على أحادي إيثانول أمين والتقليدية. نظرت الدراسة إلى ما حدث عند إضافة الماء إلى مذيب عميق سهل الانصهار مصنوع من كلوريد الكولين ومونو إيثانول أمين-(ChCl MEA DES).تم العثور على الطريقة الأكثر فعالية لامتصاص ثاني أكسيد الكربون هي الامتصاص الفيزيائي، والذي يمكن أن يحتوي على ٢٧٦,١٣ مول من ثاني أكسيد الكربون لكل جرام من DES عند ١ بار و٢٩,٠٢٥ درجة مئوية عند مزجه بالماء. يتم خلط المادة سهلة الانصهار مع الماء لزيادة كفاءة الامتصاص. تم أخذ ١٠ مل من المحلول المائي + DESs) ماء). يؤدي الجمع بين DES والماء إلى زيادة قابلية ذوبان ثاني أكسيد الكربون بشكل كبير. يمثل نموذج Design-Expert المعدل بشكل مرضي قابلية الذوبان التجريبية لثاني أكسيد الكربون في المذيب. يبلغ متوسط الفروق المئوية بين القيم التجريبية والمسقطة ١٠,٧٪ و٦,٨٪ للأنظمة الثنائية والثلاثية، على التوالي. الظروف المثالية لأقصى معدل امتصاص هي ٢٩,٠٢٥ درجة مئوية، ٢,٢٣٣ مول/لتر، و١٠١ دقيقة، مع نسبة امتصاص ٠,٠٧٣٤ مول/كجم.دقيقة وكفاءة امتصاص ٨٥,٣٪ للمحلول DES والماء.

الكلمات الدالة: امتصاص ثاني أكسيد الكربون، سهل الانصهار العميق، الطاقة، الدفيئة، البيئة.

1.INTRODUCTION

As CO2 is considered a key contributor to the greenhouse effect, the scientific community has focused on CO2 collection during the past several decades in response to growing concerns about global warming. CO2 levels topped 400 ppm for the first time in recorded history in 2013 [1], and the reduction of CO2 emissions became a prominent area of research. Thus, the most recent advancements in CO2 separation techniques were focused on removing CO2 using cost-effective technology. For additional in-depth discussions on solvents used for CO2 separation, the reader can turn to various outstanding, in-depth evaluations [1,2]. Using aqueous amine absorbents is the most well-established and commercially accepted method for CO_2 collection. Alternatives to amine-based technology have been carefully considered and deemed superior [2,3]. Nevertheless, these systems have significant limitations, including solvent deterioration, corrosion of equipment, energy-intensive solvent regeneration, and high operational costs [4]. Hence, while improvements in amine-based solvents were presented as a solution to the issues mentioned earlier, developing novel solvents for CO_2 capture with improved properties has garnered considerable interest [5]. Ionic liquids (ILs) provide new possibilities and are a viable alternative absorbent solution for improving CO_2 collection after combustion [6]. The search for new green and ecologically acceptable solvents to replace existing ones, which have drawbacks such as inherent toxicity and excessive volatility, has sparked widespread interest in ILs [7]. Many physicochemical properties of ILs, such as their low flammability, low vapor pressure, and high thermal stability, make them suitable for CO_2 collection [8]. Despite all these potential advantages, the literature reveals severe practical limits for these ILs, such as toxicity, poor biodegradability, and costly production expenses [9]. Because of their similar features and benefits, deep eutectic solvents (DESs) are gaining appeal as viable alternatives to ILs [4]. A DES is formed by mixing two or more ingredients with lower melting points than the separate constituents. DESs are typically created by combining a quaternary ammonium or phosphonium salt (a hydrogen-bond acceptor, or HBA) with one or more molecules capable of producing hydrogen bonds (a hydrogen-bond donor, or HBD). The complexation of HBD and HBA considerably decreases the freezing point of the combination. In some circumstances, DESs have notable benefits over ILs, including ease of manufacture, low cost, and biodegradability [10]. Extensive research on DES chemical and industrial applications, including biology, electrochemistry, chemical synthesis, catalysis, and material separation, has been done over the last few decades [11]. Numerous studies have shown that ionic liquids and deep eutectic solvents (DESs) may be used as CO_2 capture solvents [12]. DESs have been shown to have greater CO_2 loading than traditional ionic liquid

capture [13]. However, CO_2 solubility data are scarce for DESs, prompting more studies to design novel gas absorbents. Recent research [14] presented a novel class of DESs with relatively high CO_2 uptake, accomplished using ethylenediamine (EDA) as a hydrogen-bond donor (HBD) and monoethanolamide hydrochloride as a hydrogen-bond acceptor (HBA), created by adding hydrogen chloride (HCl) to monoethanolamine (MEA). This combination has the highest CO_2 loading value of any current DES. A similar study has indicated that DESs are viable replacements for standard monoethanolamine-based solvents utilized in cleaning technologies [5]. DES's creation depends on the intensity of the interaction between its constituent parts. Fig. 1 illustrates the interaction between A and B. In theory, unlike perfect mixtures, these interactions result in a significant value of freezing point ΔT_f. The eutectic point is reached at a specific temperature when the amount of A to B is just right. At this time, the melting point, the depression seen in Fig. 1 [15], is detected.

As seen in Table 1, DES may be broadly categorized into four main groups. The cation indicated as CAT+ in the table in type III DES is commonly quaternary ammonium, phosphonium, or sulfonium salt. The anionic component, designated by the symbol x-, forms hydrogen bonds with the protons of the RZ donor group [1]. Choline Chloride is a popular quaternary ammonium salt due to its cost, accessibility, biodegradability, and low toxicity. Hydrogen bonding makes it easier for the chloride anion to interact with diverse proton donors [2,3].

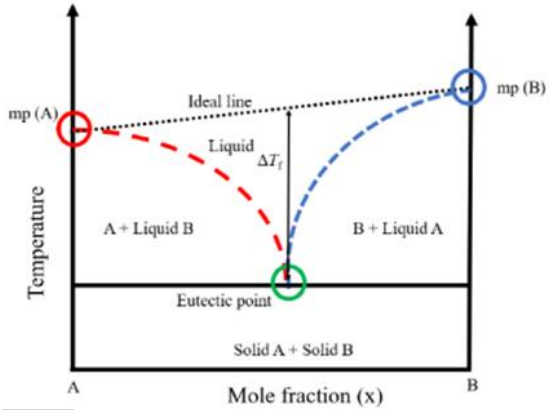

Fig. 1 T-X diagram for DES. Adopted from [8].

Table 1 General Formula for DES Classification, Adopted from [9].

Type	General Formula	Terms
Type I	$Cat^+X^-zMCL_x$	M= Zn,Sn, Sl, Ga, In
Type II	$Cat^+X^-zMCL_x.yH_2O$	M= Cr, Co, Cu, Ni, Fe
Type III	Cat^+X^-RZ	Z= $CONH_2$, COOH, OH
Type IV	$MCl_x + RZ = MCl^+_{x+1}.RZ + MCl^-_{x+1}$	M= Al, Zn and Z= $CONH$, OH

As previously stated, DES is synthesized by combining a hydrogen bond donor (HBD) with a hydrogen bond acceptor (HBA). Various combinations could provide desirable physicochemical qualities, such as conductivity, viscosity, polarity, and thermal properties. The required qualities may be obtained by adjusting the molar ratios of the components, and it is worth mentioning that the bulk of the produced DESs have hydrophobic properties [3]. Therefore, the novelty in the present work is represented in the use of a new type of eutectic solvent with new molar ratios to provide desirable physical properties of the solvent to enhance CO_2 capture that have not been previously discussed in the research and compared with the results of other researchers' research who used ionic solvents under similar conditions. This study aims to capture CO_2 from simulation gas (CO_2, N_2) using a deep eutectic solvent (DES), namely a 1-ChCl-6MEA mixture, through an experiment of cell absorption. This work investigates the absorption efficiency of CO_2 from gas with different parameters to find the best operating conditions of absorption, which include solvent concentration, temperature, and reaction time, using amine-based solvents alone and comparing them with eutectic solvents and determining the best of them, also comparing DES with ionic liquids to find the best loading of CO_2.

Choline Chloride

2-Hydroxy-ethyl-tri-methyl-ammonium cation or $HOCH_2CH_2N^+(CH_3)_3$, commonly known as choline chloride, has a structure, as shown in Fig. 2. Choline chloride is biodegradable, non-toxic, and cheap to manufacture. It has been defined as a pro-vitamin in Europe. It is made on a massive scale as an animal feed addition, reaching mega-ton volumes. A single-step gas-phase reaction involving HCl, ethylene oxide, and tri-methyl-amine is used in the manufacturing process. This technique produces very little extra waste [5]. Except for the composition temperature, heat capacity, and ecotoxicity, many of the features of choline-based DESs are identical to those of ordinary ILs. These solvents' reduced heat capacity contributes to less sensible heat with increasing temperature, resulting in lower energy use in the CO_2 extraction process. The non-ecotoxicity, biodegradability, and low cost of choline chloride-based DES indicate an excellent use for an alternative eco-friendly CO_2 capture medium [10]. Choline chloride is the primary focus of this work; choline chloride-based DES has shown great potential for CO_2 adsorption with good electrical conductivity, which is suitable for electrochemical conversion because of lower ohmic losses. Amine-based DES has also been considered for the study due to higher CO_2 absorption.

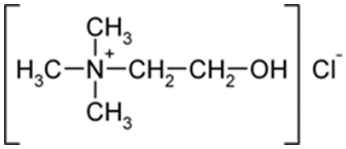

Fig. 2 Chemical Structure of Choline Chloride.

2.EXPERIMENTAL PART

2.1.Materials

Choline chloride (AR, 98%) and monoethanolamine (AR, 99%) were purchased from Aladdin Pharma Co. CO_2 gas (99.99%) and N_2 (99.999%) were purchased from Guizhou Sanhe Gas Co., Ltd., China.

2.2. Equipment

The equipment used in this work is listed in Table 2.

2.3.Solvent Preparation

The DES composition utilized in this experiment was a 1:6 mol ratio of Choline Chloride (ChCl) and Monoethanolamine (MEA). This mole ratio was selected based on its successful synthesis and the ideal balance of ChCl and MEA, according to Li et al. [21,22], who discovered that a mole ratio of 1:6 was optimum among the ChCl to MEA ratios of 1:2 to 1:5. Fig. 3 shows the structure of choline chloride monoethanolamine DES (a) and crystallization in a ChCl:MEA (1:6) mixture (b). To make the DES, the required amounts of ChCl and MEA were individually weighed and mixed to obtain the requisite 1:6 mole ratio. After that, the mixture was transferred to a beaker and set on a magnetic hot plate with a stirrer. The liquid was heated to 60 °C and then agitated at 300 revolutions per minute for three hours. The resulting clear, white, and uniform liquid was bottled and allowed to settle undisturbed for 48 hours. If the DES demonstrated phase stability throughout this period, it was used in further experiments.

2.4.Fourier Transform Infrared Spectroscopy (FTIR)

Figure 4 depicts the Fourier-Transform Infrared Spectroscopy (FTIR) setup. This apparatus is used to detect distinct bonds in the solvent and how and when new bonds form, producing diverse compounds. The equipment emits infrared radiation ranging from 10,000 to 100 cm^{-1} through the material. Some of the radiations are absorbed, while others pass through. Radiation received by molecules is transformed into rotation and/or vibration energy. The integrated data logger supports traceability and provides complete documentation (HACCP/IFS/ISO) model atmocheck DOUBLE O_2/CO_2/ U.S.A. The resultant signal from the detector is shown as an absorption spectrum. For this specific machine, the wavenumbers in the spectrum are from 4000 to 400 cm^{-1}. The spectrum generated is a series function of absorbed energy. This machine uses a zinc selenide crystal, providing more durability at the cost of minor errors. For higher resolution, germanium crystal could be used. This experimental setup measures 16 iterations per sample and the resolution of 2 cm^{-1}.

Table 2 List of Tools and Devices Used in this Work.

No.	Equipment/Facilities	Model	Properties	Purpose of use
1	Hot plate stirrer	Labtech/ Korea	60 – rpm Max. temperature 380 °C	Analytic and preparation
2	Analytical balance	OHAUS /U.S.A	Readability 0.0001 g	Preparation
3	Glass flask	Glassco /India	100ml	Desorption
4	Glass condenser	Glassco /India		Desorption
5	Flow meter	Flowtech /U.S.A	Air (25 -250) ml/min CO_2 (25-250) ml/min	Absorption
6	Thermometer	Germany	Mercury (0 – 200) °C	Desorption
7	Absorber cell	India	50 ml	Absorption
8	CO_2 analyzer	Atmocheck DOUBLE O_2/CO_2/ U.S.A	Range (0.00 – 100) %	Analysis
9	Water bath	England	Cooling/heating range -15°C to 200°C	Analytic and preparation
10	Pressure gauge	Visto/German	Range (0 – 50) bar	Pressure gauge

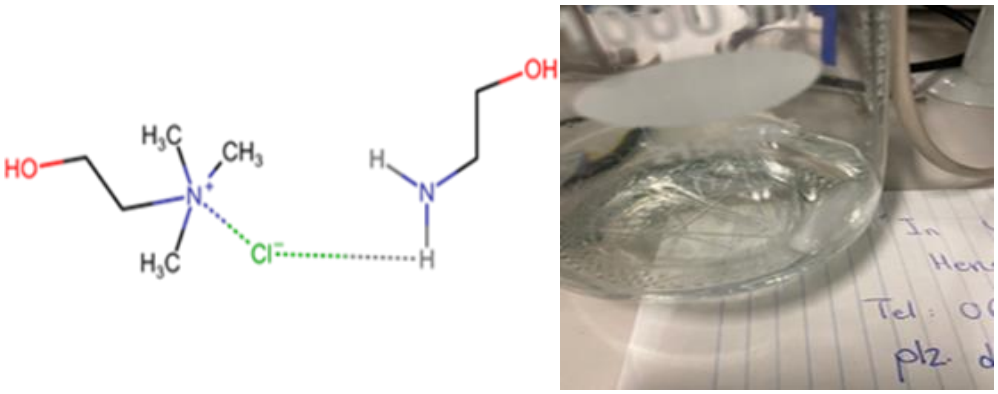

(a) DES Structure **(b)** Crystals in ChCl:MEA

Fig. 3 (a) ChCl:MEA(1:6) DES Structure (b) Crystals in ChCl:MEA(1:6) [11].

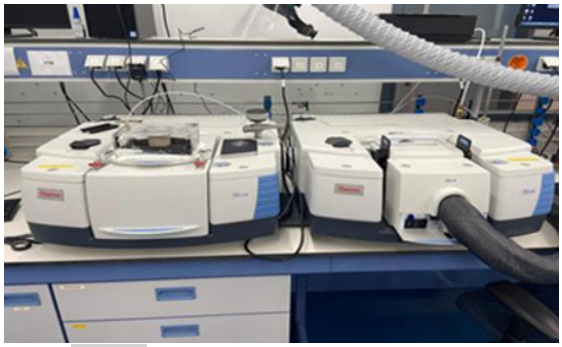

Fig. 4 Nicolet iS50 FT-IR Machine.

2.5.CO_2 Analysis

The CO_2 analyzer is used to assess the entrance and output concentrations of CO_2 gas in the absorption cell, determining the saturation of the solvent and the endpoint of the CO_2 absorption procedure. Excels with easy operation, short measuring times, and low gas volume sample requirement. The integrated data logger supports traceability and provides complete documentation (HACCP/IFS/ISO) model atmocheck DOUBLE O_2/CO_2/ U.S.A. The CO_2 analyzer is shown in Fig. 5.

Fig. 5 The CO_2 Analyzer Apparatus.

The CO_2 absorption rate by the deep eutectic solvent is the difference in CO_2 gas rate between the inlet and outlet of the absorber from the gas phase [12, 13], as calculated from:

$$r = \frac{Qin - Qout}{m * 22.4 * 1000} \quad \textbf{(1)}$$

where:

r: The absorption rate of the CO_2 (mol/kg. min).

Q_{in}: The inlet gas flow rate (ml/min).

Q_{out}: The outlet gas flow rate (ml/min).

m: The quantity of the solvent (kg).

22.4: A conversion (mol/l).

The CO_2 absorption loading can be calculated from [12]:

$$C_T = r * t \quad \textbf{(2)}$$

where:

C_T: The absorption loading of the solvent (mol/kg).

r: The absorption rate of the CO_2 (mol/kg. min).

t: The time of absorption (min).

Absorption capacity (AC) was calculated from [14]:

$$AC = C_T \times MW._{CO_2} \times 1000/1000 \quad \textbf{(3)}$$

Where:

MW.: Molecular weight of CO_2.

Solubility (Xg) of CO_2 in solvent calculated from [15]:

$$Xg = \frac{\text{mole of} CO_2}{\text{mole of} CO_2 + \text{total mole of solution}} \quad \textbf{(4)}$$

2.6.Design Expert Software

Design Expert Software was used in this study to plan the tests, optimize the system, and evaluate how well it worked. Both process variables and combination variables are manipulable by Design-Expert software. The following are the three essential components of a design expert:

i. To build the design, it is necessary to determine the answers and the most important parts and then do the tests according to the design table. These elements are shown in Table 3.

ii. After the real answer facts have been entered, the model can be analyzed. It consists of design diagnostics utilizing ANOVA, normal distribution plots, and actual vs. expected plots. System design and mathematical modeling also provide model graphs to depict outcomes, such as interactions, 3-D surfaces, contours, one-factor systems, and cubes.

iii. To optimize a process, each answer must be evaluated to develop a good model. Then, one response can be optimized graphically or mathematically, or many can be optimized simultaneously. Table 3 shows the test spectrum and the levels of the independent absorption process parameters.

Table 3 Measured Range and Dimensions of Independent [1-CHCL] [6-MEA] Components in the Absorption.

Name	Units	Low	High	-alpha	+alpha
Temperature of solvent	°C	25	45	25	45
Concentration	mole/l	0	3	0	3
Absorption time	Min	60	120	60	120

2.7.Experimental Procedure

Before the experiment, 1-choline chloride and 6-monoethanolamine were used as deep eutectic substances at concentrations of (0-3) mol/L and temperatures of (25-45) °C.

To boost the absorption effectiveness, the deep eutectic is combined with water. 10 milliliters of the solution (DESs + water) were withdrawn. The monoethanolamine solvent alone was also used to be compared with the deep eutectic solvents with a fixed concentration (4 mol/L) and different temperatures (25-45) °C, which enabled to come into touch with the solution to absorb carbon dioxide CO_2 was pumped from the feeding tank first through the flow meters used It is installed inside the system to measure its concentration in advance before entering it into the absorption cell to ensure the required percentage of it in the experiment using a carbon dioxide analyzer. Five or more

measurements were performed at different time intervals to ensure the stability of the outside percentage of carbon dioxide to the required temperature after the arrival of the water bath. Then, Carbon dioxide and nitrogen gas were passed to the absorption cell and the solution to cause the absorption process. The carbon dioxide and nitrogen flow rate was maintained to ensure the accuracy of the measurements read by the carbon dioxide analyzer, as a measurement was taken after five minutes throughout the entire experiment period by the carbon dioxide analyzer. In this study, the run time (60 to 120 min) was tracked when a carbon dioxide analyzer showed a significant change in the amount of carbon dioxide. Figs. (6, 7) depict the experiments for the adsorption step utilized in this study, respectively. After the liquid ring was set correctly, the carbon dioxide gas was pumped from the gas cylinder through the preset tube and valve to direct the gas stream directly into the carbon dioxide absorption cell, adjusted to the desired level. It must be noted here that the above experimental procedure was applied in this study for all absorbances for the two solvents, once with monoethanolamine alone and once with the solution containing (DESs+H_2O), where their results were compared.

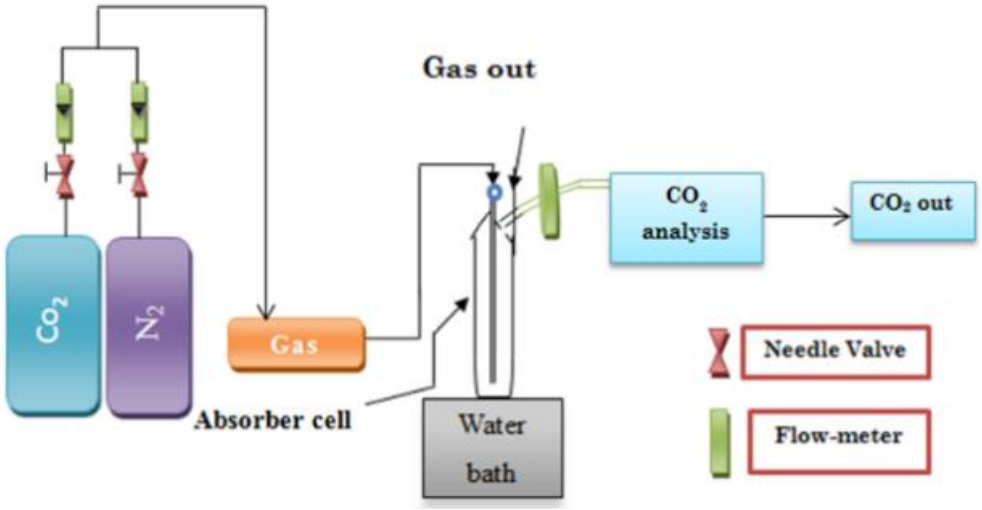

Fig. 6 The Schematic Diagram for CO_2 Absorption.

Fig. 7 Photograph of the Whole Experimental Setup.

3.THE RESULTS OF CENTRAL COMPOSITE DESIGN MODEL

Batch testing supported revising the central composite design (CCD) of the key factors influencing parameter computation (CO_2 outlet, absorption rate, CO_2 loading, and CO_2 capacity and solubility). The mathematical equations used to forecast the parameters were found by analyzing the findings of the solvents using design expert software (DE). The Response Surface Method (RSM), a widely used statistical technique for designing experiments across various engineering and research fields, was employed in this study. A three-core compound design (CCD) was used to examine the impacts of independent variables (solvent temperature, concentration, and absorption time). Twenty experimental runs, five repeated at the center spots, were necessary for each approach. The Design-Expert 11 software was used for the trials. The computer software suggests a quadratic model to derive the response regression equation from the experimental data in Table 4. Eqs. (5) - (9) for

the solvent [1-chcl], [6-MEA] are a list of all computational parameters of the response equation that were used to forecast parameters in cryptographic object relationships.
For sample, the following Eq.: -

CO_2 outlet rate = +5.71 - 0.5400*A_1 + 4.15*B_1 + 2.88*C_1 + 0.0625*A_1B_1 - 0.0875*A_1C_1 + 1.91*B_1C_1 + 4.33*A_1^2 – 1.92*B_1^2 - 1.97*C_1^2 **(5)**

Absorption rate = +0.0537+0.0034*A_1 - 0.0257*B_1 - 0.0167*C_1 -0.0007*A_1B_1 + 0.0007*A_1C_1 - 0.0107*B_1C_1- 0.0251*A_1^2+0.0130*B_1^2+0.0111*C_1^2 **(6)**

CO_2 loading = +4.87+0.3209*A_1 - 2.57*B_1 + 0.1509*C_1 -0.2099*A_1B_1 + 0.2316*A_1C_1 - 1.71*B_1C_1- 2.35*A_1^2+1.08*B_1^2+0.5996*C_1^2 **(7)**

CO_2 capacity = +214.19 +14.12*A_1 - 112.93*B_1 + 6.64*C_1 -9.24*A_1B_1 + 10.19*A_1C_1 - 75.07*$B_1C_1$103.24*A_1^2+47.63*B_1^2+26.38 *C_1^N2 **(8)**

Solubility = + 0.1226 + 0.0126*A1 - 0.0155*B1 + 0.0022*C1 - 0.0299*A_1B_1 +0.0009*A_1C_1 - 0.0013*B_1C_1 - 0.0127*A_1^2 - 0.0587*B_1^2 -0.0014C_1^2 **(9)**

Where:
A: Temperature of solvent (°C)
B: Concentration (mol/l)
C: Absorption time (Min)

3.1.Visual Model Analysis Using 2D Contour Plots and a 3D Response Surface for the Third Sample [1-Chcl] [6-MEA]

A 3D response surface perimeter (3D) map highlights the influence of the independent variable on the response. The type of interaction between the explanatory components is indicated by 2D contour plots. If the form is oval or curved, the variables do not interact [11]. complexity or the geometry of the beam. Therefore, the necessity for internal reinforcing through straightforward mechanisms was created. Placing an interior cross-rod (CR) within the beams is suitable. The novel concept is to use this technique to enhance the torsion resistance of reinforced concrete, placing an interior cross-rod inside the beams.

Table 4 Experimental Data Points and Response Used in Central Composite Design (CCD).

Std.	Run	Factor 1 **A: Temp.** °C	Factor 2 **B: Conc.** mol/l	Factor 3 **C: Time** min	Response 1 **Co_2 outlet %** %	Response 2 **Absorption rate** mol/kg.min	Response 3 **CO_2 loading** mol/kg	Response 4 **CO_2 capacity** mgco2/g solv.	Response5 **Solubility** mole CO2/mole
13	1	35	1.5	60	3.4	0.0665	3.99	175.56	0.1323
8	2	45	3	120	14.7	0.00173	0.208	9.152	0.0399
2	3	45	0	60	0.5	0.0875	5.25	231	0.1267
17	4	35	1.5	90	4.7	0.0595	5.355	235.62	0.1131
18	5	35	1.5	90	4.7	0.0595	5.355	235.62	0.1131
9	6	25	1.5	90	10.6	0.0251	2.259	99.396	0.1208
6	7	45	0	120	1.1	0.0839	10.068	442.992	0.1267
4	8	45	3	60	3.1	0.0682	4.092	180.048	0.0384
1	9	25	0	60	0.6	0.0866	5.196	228.624	0.05
3	10	25	3	60	6.3	0.05	3	132	0.0775
19	11	35	1.5	90	4.7	0.0595	5.355	235.62	0.1131
14	12	35	1.5	120	7.1	0.0457	5.484	241.296	0.1442
5	13	25	0	120	4.9	0.06	7.21	317.24	0.05
12	14	35	3	90	10.1	0.0285	2.565	112.86	0.0563
11	15	35	0	90	0.5	0.0875	7.875	346.5	0.1
16	16	35	1.5	90	4.7	0.0595	5.355	235.62	0.1131
7	17	25	3	120	14.9	0.00056	0.0672	2.9568	0.0863
10	18	45	1.5	90	12.5	0.0147	1.323	58.212	0.1784
15	19	35	1.5	90	4.7	0.0595	5.355	235.62	0.1131
20	20	35	1.5	90	4.7	0.0595	5.355	235.62	0.1131

3.1.1.Effect of Temperature and Concentration on the CO_2 Outlet Concentration

The chemical absorption is attributed to the ability of the choline chloride to form hydrogen bonds with the amines. Fig.8 shows that the solubility of CO_2 increased with the molar ratio of amine in the DES [13,14]. For example, at a temperature of 35˚C and concentration of 1.5 mol/l, the CO_2 outlet was 7.1 vol.%. Nevertheless, the temperature was 45 ˚C, the concentration was 3mol/l, and the CO_2 outlet was 14.9 vol.% at the constant time.

3.1.2.Effect of Temperature and Time on the CO_2 Outlet Concentration

Figure 9 shows that the CO_2 outlet concentration increased with temperature and time due to higher temperature leading to a higher reaction rate constant and, consequently, higher mass transfer rate and decreased absorption efficiency [18]. For example, at a temperature of 35˚C and after 60 minutes, the CO_2 outlet was 3.4 vol.%; however, at a temperature of 45˚C and after 90 minutes, the CO_2 outlet was 12.5 vol.% at a constant concentration.

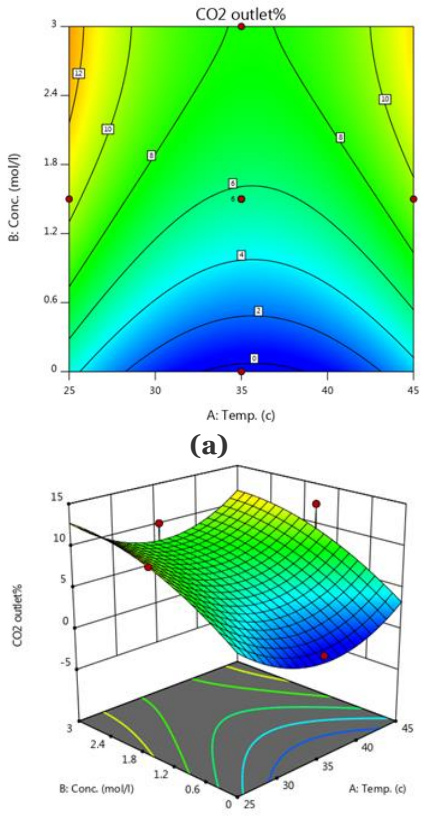

Fig. 8 Effect of Temperature and Concentration on the CO_2 Outlet Concentration, (a) 2D Counter Plot and (b) 3D Plot.

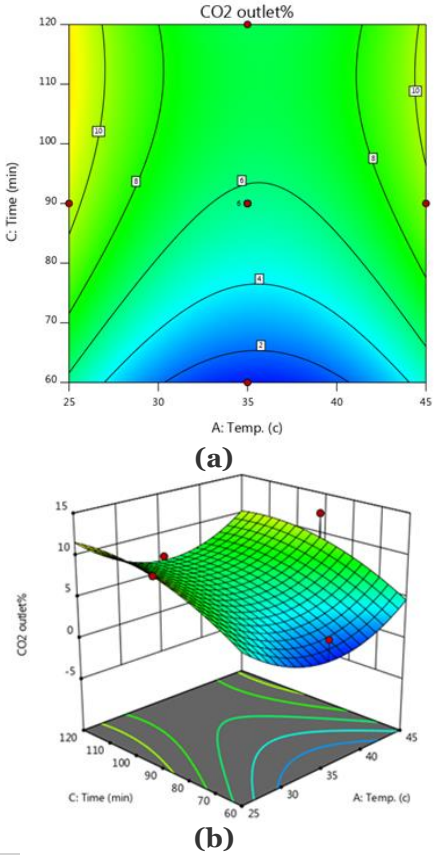

Fig. 9 Effect of Temperature and Time on the CO_2 Outlet Concentration, (a) 2D Counter Plot, and (b) 3D Plot.

3.1.3.Effect of Concentration and Time on the CO_2 Outlet Concentration

Figure 10 shows the effect of concentration and time on the CO_2 outlet concentration. This observation can be explained by one reason. All DESs studied could be observed to have good stability at a temperature of 35˚C, where the regeneration process was conducted. Moreover, the MEA-based DESs exhibited better stability than the phenol-based DESs. Increasing the solvent content additionally elevated viscosity, which in many situations hampers the liquid's ability [13]. For instance, at 1.5mol/l and following 60 minutes, the CO_2 outflow was 3.4 vol.%. However, at 3mol/l and after 90 minutes at a steady temperature, the CO_2 outlet was 10.1 vol.%.

3.1.4.Effect of Temperature and Concentration on the CO_2 Absorption Rate

Figure 11 shows that the absorption rate decreased when the temperature and concentration of the deep eutectic solvent [1-chcl] [6-MEA] increased. It results from the interaction between CO_2 molecules and DESs, in which the CO_2 molecules occupy the "free space." A significant quadrupole moment and Van der Waals forces were used inside the DESs structure [13]. For example, at 35 °C and 1.5 mol/l level, the absorbing velocity was 0.06650 mol/kg.min, whereas at 45 °C and 3 mol/l concentration, the absorbance value was 0.000173 mol/kg.min.

3.1.5.The Impact of Temperature and Time on CO2 Absorption Rate

At a fixed concentration, the absorption rate decreased with increasing duration and temperature, as illustrated in Fig.12, due to the capacity of the exothermic CO_2 absorption thermodynamics system to generate reversible responses [14]. As an illustration, at 25°C and after 90 minutes, the absorption rate was 0.0682 mol/kg.min; however, when the temperature was raised to 35 °C, and after 120 minutes with fixed concentration, the absorbance level was 0.0441 mol/kg.min.

3.1.6.Effect of Time and Concentration on the CO_2 Absorption Rate

As shown in Fig.13, the process of absorption efficiency declined with time and increased with increasing the solvent content at a constant temperature. This decrease might be because raising the amount of solvent made the liquid thicker, making it more difficult to spread and delaying the mass transfer [18]. The absorption rate was 0.0682 mol/kg.min after 90 minutes at a concentration of 1.5mol/l. Nonetheless, after 120 minutes at a constant temperature and a concentration of 3mol/l, the absorption rate was 0.025 mol/kg.min.

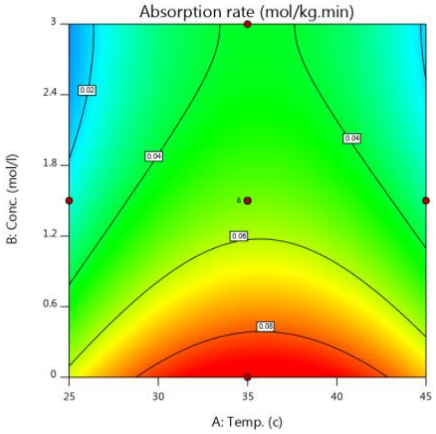

(a)

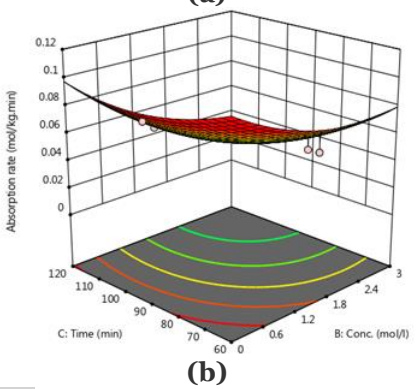

(b)

Fig. 10 Effect of Concentration and Time on the CO_2 Outlet Concentration, (a) 2D Counter Plot, and (b) 3D Plot.

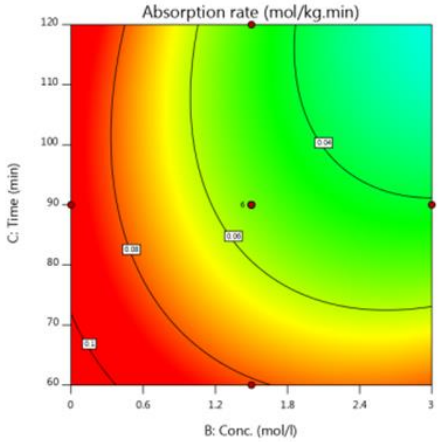

(a)

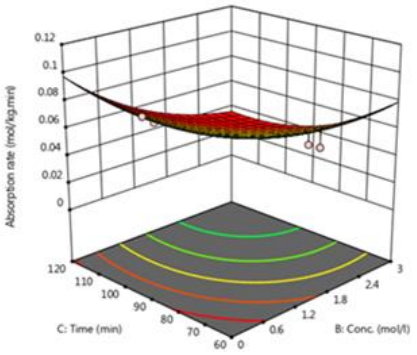

(b)

Fig. 12 Effect of Temperature and Time on the CO_2 Absorption Rate, (a) 2D Counter Plot, and (b) 3D Plot.

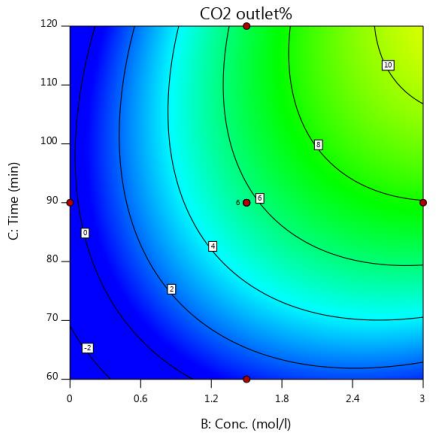

(a)

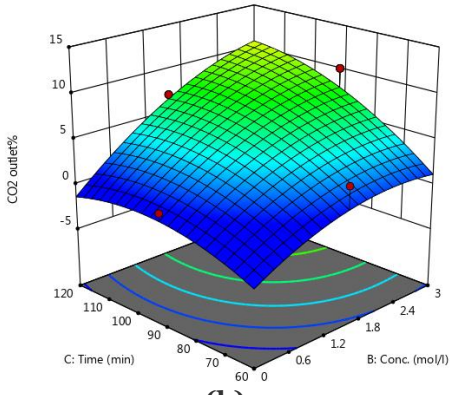

(b)

Fig. 11 Effect of Temperature and Concentration on the CO_2 Absorption Rate, (a) 2D Counter Plot and (b) 3D Plot.

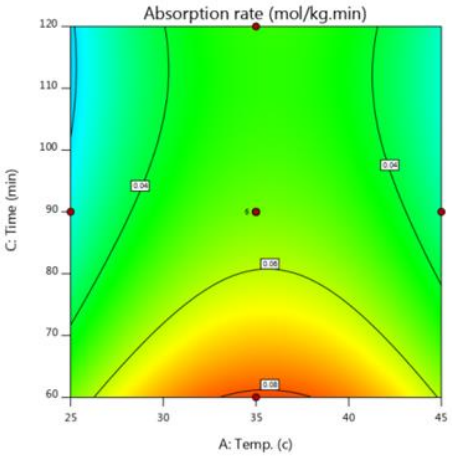

(a)

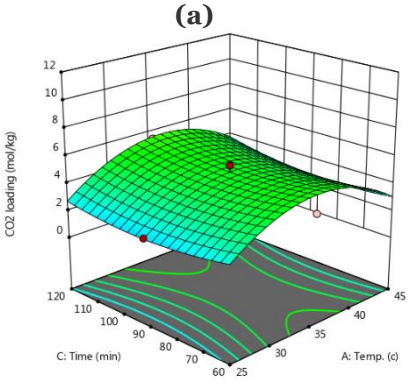

(b)

Fig. 13 Effect of Concentration and Time on the CO_2 Absorption Rate (a) 2D Counter Plot and (b) 3D Plot.

3.1.7.Effect of Temperature and Concentration on the CO_2 Loading

Carbon dioxide loading the solution was the most influential process parameter on the overall mass transfer coefficient compared to the temperature and concentration of the solvent. The loading of CO_2 decreased with increasing temperature and solvent concentration, as shown in Fig.14, because of the active absorbent (MEA) concentration; the lower its concentration, the higher the CO_2 loading [19]. For instance, at 35 °C with an average concentration of 1.5mol/l, the amount being loaded of CO_2 was 5.355mol/kg, whereas, at 45 °C and a density of 3 mol/l, the loading of CO_2 was 4.092 mol/kg.

3.1.8.Effect of Temperature and Time on the CO_2 Loading

Figure 15 shows that the CO_2 loading increased as time and temperature decreased because the chemical reaction involving MEA caused greater CO_2 loading. This phenomenon may be attributed to its existence. For example, at 45 °C and 105 minutes, the CO_2 loading reached 8.243 mol/kg. Meanwhile, at 35 °C and 120 minutes, the CO_2 loading was 6.613 mol/kg while keeping a steady concentration [15].

3.1.9.The Influence of Concentration and Time on CO2 Loading

Figure 16 shows CO_2 loading decreased as time and solvent concentration rose. This finding might be attributable to a lack of water content at high concentrations of [1-chcl] [6-MEA] [16]. For example, at a concentration of 1.5 mol/l for 60 minutes, the CO_2 loading was 3.99 mol/kg. The CO_2 loading dropped to 2.565 mol/kg at a concentration of 3 mol/l, a period of 90 minutes, and a constant temperature.

3.1.10.Effect of Temperature and Concentration on the CO_2 Absorption Capacity

The absorption capacity decreased with increasing the temperature and solvent content, as seen in Fig.17, demonstrating the presence of parallel physical and chemical absorbance processes [13]. For example, at 35 °C and a concentration of 1.5 mol/l, the absorption capacity was 175.56 mg CO_2/gm solvent. Nevertheless, at 45°C and 3 mol/l levels, the absorption capacity reduced to 170.882 mg CO_2/gm solvent.

3.1.11.Effect of Temperature and Time on the CO_2 Absorption Capacity

The absorption capacity declined with increasing time and temperature due to a drop-in absorption rate, as illustrated in Fig.18, due to replacing the acidic hydrogen on the C_2 carbon of the [MEA] cation with a methyl group and changing the organization of the anion and CO_2 a little in comparison to the cation. For example, at 25 °C and 60 minutes, the absorption capacity was 132 mg CO_2/gm solvent. However, at 35 °C and 90 minutes, the absorbance rate was 112.68 mg CO_2/gm solvent with a constant level [17].

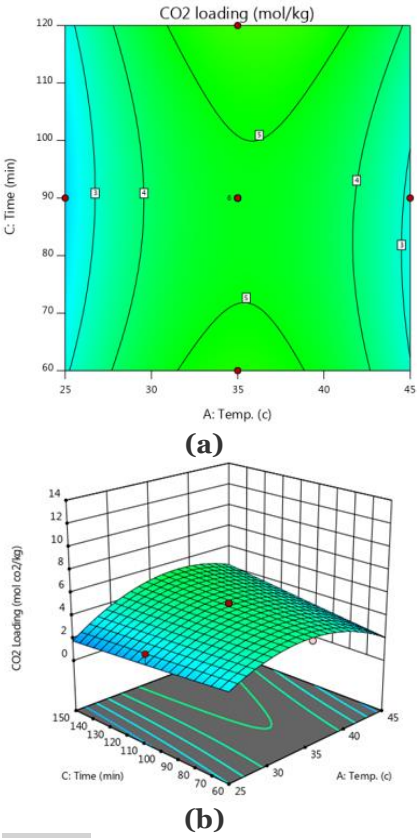

(a)

(b)

Fig. 14 Effect of Temperature and Concentration on the CO_2 Loading, (a) 2D Counter Plot, and (b) 3D Plot.

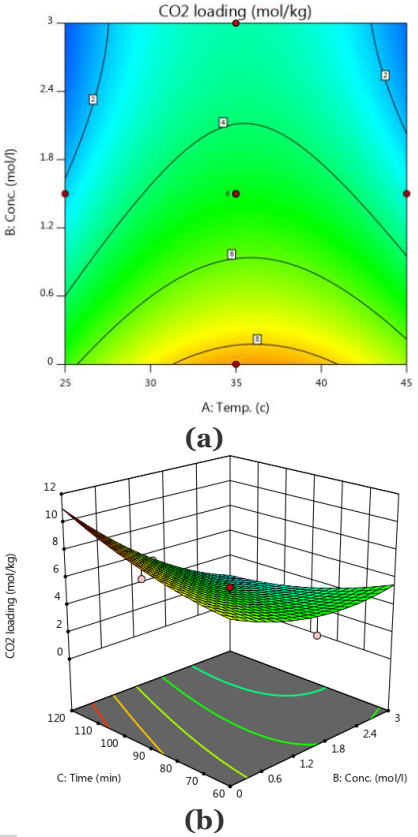

(a)

(b)

Fig. 15 Effect of Temperature and Time on the CO_2 Loading, (a) 2D Counter Plot, and (b) 3D Plot.

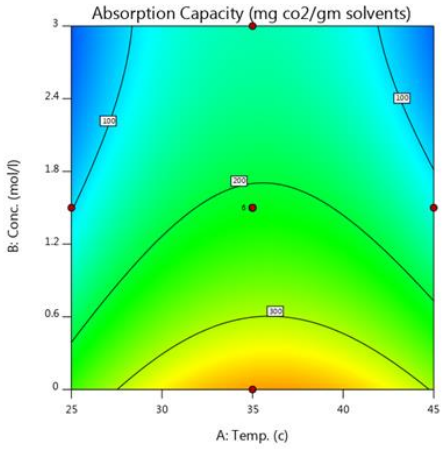

(a)

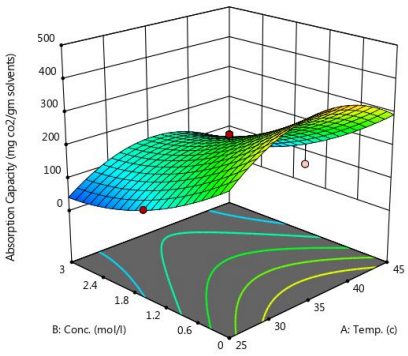

(b)

Fig. 16 Effect of Concentration and Time on the CO_2 Loading, (a) 2D Counter Plot, and (b) 3D Plot.

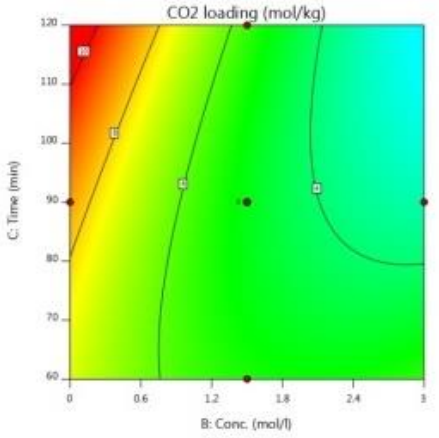

(a)

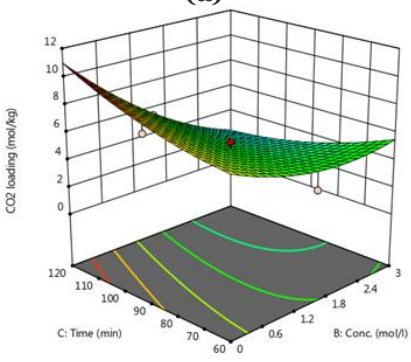

(b)

Fig. 17 Effect of the Temperature and Concentration on the CO_2 Absorption Capacity, (a) 2D Counter Plot, and (b) 3D Plot.

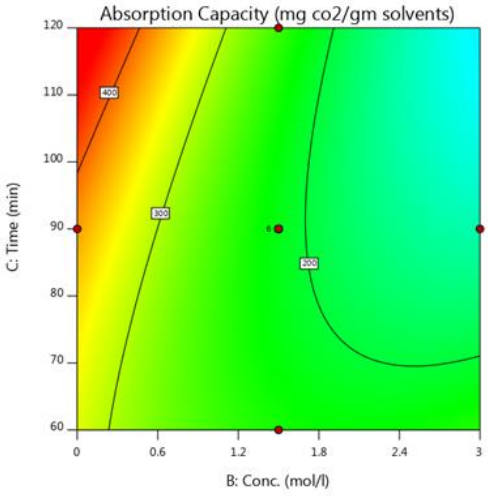

(a)

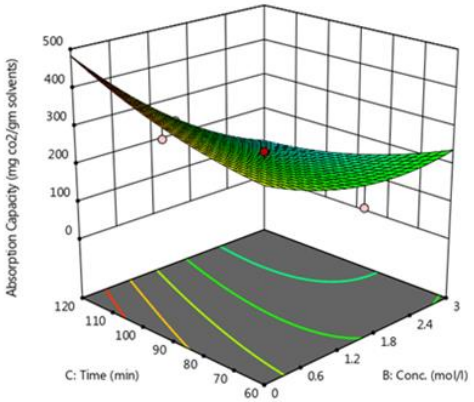

(b)

Fig. 18 Effect of the Temperature and Time on the CO_2 Absorption Capacity, (a) 2D Counter Plot, and (b) 3D Plot.

3.1.12.The Impact of Concentration and Time on the Capacity of CO_2 Absorption

As shown in Fig.19, the capacity for absorption reduced as the solvent content increased due to a reduction in absorption rate [18]. For illustration, at 1.5mol/l and after 90 minutes, the rate of absorption capability was 99.396 mg CO_2/gm solvent. In contrast, at 3mol/l and after 120 minutes at the same temperature, the absorbing capacity was 9.152 mg CO_2/gm liquid.

3.1.13.Effect of Temperature and Concentration on the CO_2 Solubility

The solubility decreased with increasing the temperature and solvent concentration, as shown in Fig. 20. The choline chloride's capacity to create hydrogen bonds with the amines caused the chemical absorption. As the molar ratio of amine in the DES rose, the solubility nature of the quantity of CO_2 also increased. This increase makes sense because the possibility of a hydrogen bond network developing with the choline chloride increased with the amine concentration [13]. At 25°C and 1.5mol/l concentration, a measure of dissolving was 0.0469 mole CO_2/mole. However, at 35°C and 3mol/l level, the steady-state solubility was 0.0409 mole CO_2/mole.

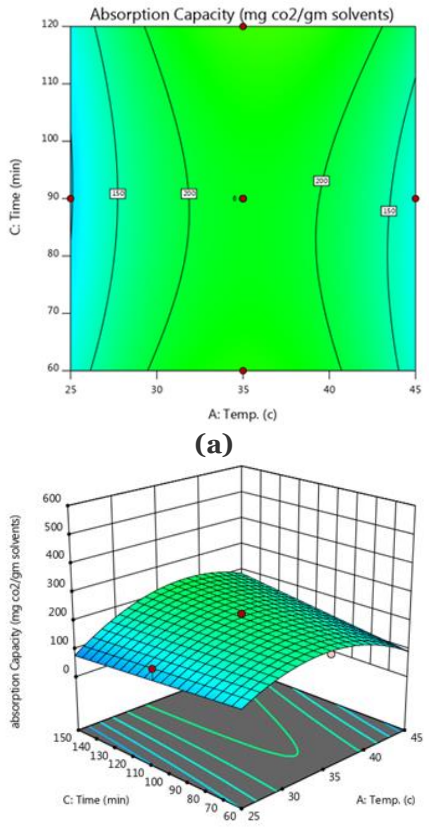

Fig. 19 Effect of the Concentration and Time on the CO_2 Absorption Capacity, (a) 2D Counter Plot, and (b) 3D Plot.

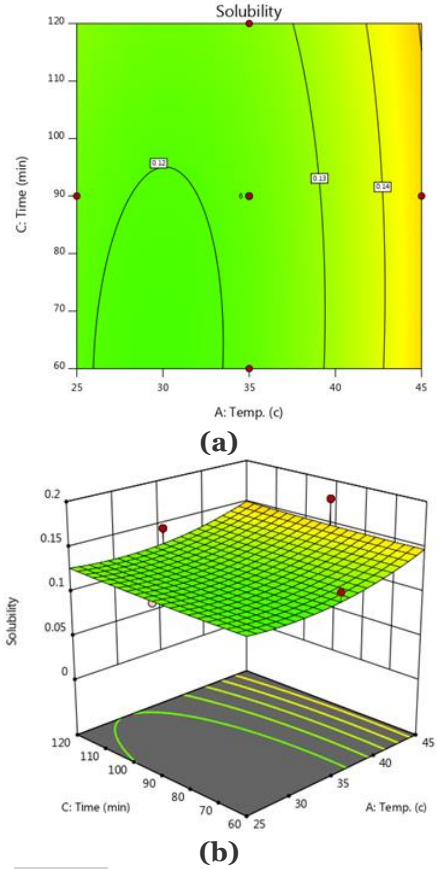

Fig. 20 Effect of Temperature and Concentration on the Solubility, (a) 2D Counter Plot, and (b) 3D Plot.

3.1.14.The Impact of Time and Temperature on the CO_2 Solubility

Figure 21 shows that solubility increased with time and temperature. The CO_2 solubility increased with the molar ratio of MEA in the DES. This relationship can be explained by increasing the MEA concentrations, resulting in stronger chemical and physical CO_2 absorption [7]. For example, at 25 °C and 90 minutes, the solubility reached 0.0469 mole CO_2/mole. However, after 120 minutes at 35 °C at a steady concentration, the solubility improved to 0.055 mole CO_2/mole.

3.1.15.The Impact of Time and Concentration on the CO_2 Solubility

Solubility declined with increasing time and the solvent content, as shown in Fig.22. It was found that when the molar ratio of the amine in the DES rose, the solubility of CO_2 [19] also increased. For example, at a concentration of 1.5 mol/l for 60 minutes, the solubility was 0.0469 mole CO_2/mole. Nevertheless, at a concentration of 3 mol/l at a steady temperature for 90 minutes, the solubility dropped to 0.0409 mole CO_2/mole.

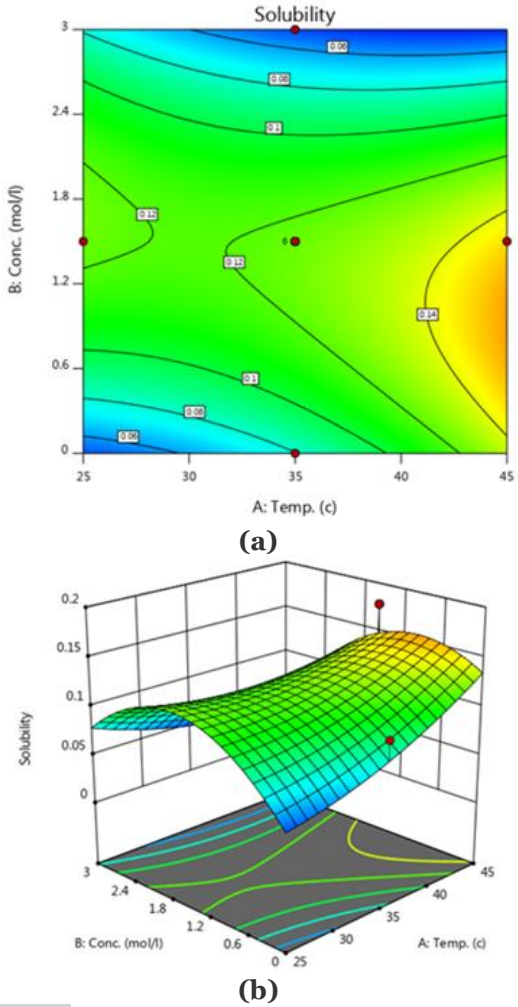

Fig. 21 Effect of Temperature and Time on the CO_2 Solubility, (a) 2D Counter Plot, and (b) 3D Plot.

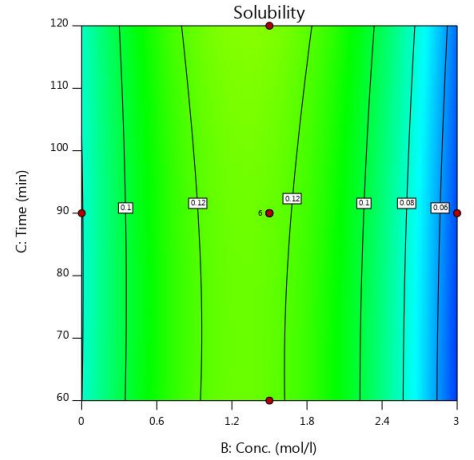

(a)

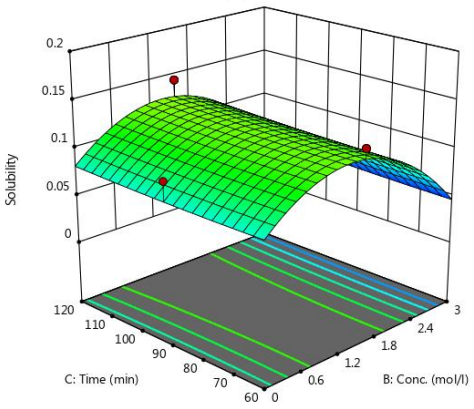

(b)

Fig. 22 Effect of Concentration and Time on the CO_2 Solubility, (a) 2D Counter Plot, and(b) 3D Plot.

3.2.Fourier Transform Infrared Spectroscopy (FTIR)

3.2.1.FT-IR Spectra of [1-CHCL] [6-MEA] Before Absorption Process

Fig. 23 highlights how the physico-chemical interaction of 1-ChCl-6-MEA changed the FT-IR spectrum response between the pure substances and the produced eutectic. The vibrations of hydrogen bonds of the types O-H, N-H, and/or O-H•O and/or N-H•O were observed between 3352 and 3355 cm^{-1} [20], indicating the presence of molecular aggregation unique to eutectic mixtures. In the case of deep eutectic, this spectral band was maximum at 3358–3397 cm^{-1}, which belongs to the –NH group, and at 3329–3328 cm^{-1}, which belongs to hydrogen bonds. The vibration bands at 1660 cm^{-1}, 1656 cm^{-1}, and 1607 cm^{-1} were likewise associated with these. The HO HN group from 924 cm^{-1} is present in Fig.23.

3.2.2.FT-IR Spectra of [1-CHCL] [6-MEA] After Absorption Process

Fig. 24 shows the FTIR spectrum for ChCl:MEA (1:6) solution with concentration of CO_2. As discussed previously, MEA reacted with CO_2 to form carbamates, as shown in Fig.24. In the FTIR spectrum, the carbamate bond peak was observed at 1322 cm^{-1} [21]. In ChCl:MEA DES, the peak was observed at 1307 cm^{-1}, as shown in Fig.24. The peak at 1307 cm^{-1} increased with the concentration of CO_2.

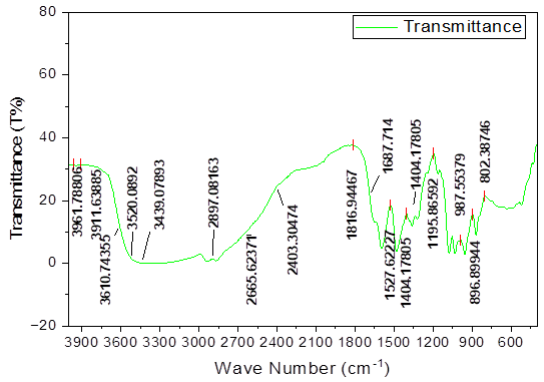

Fig. 23 FT-IR Spectra of [1-CHCL] [6-MEA] Before Absorption.

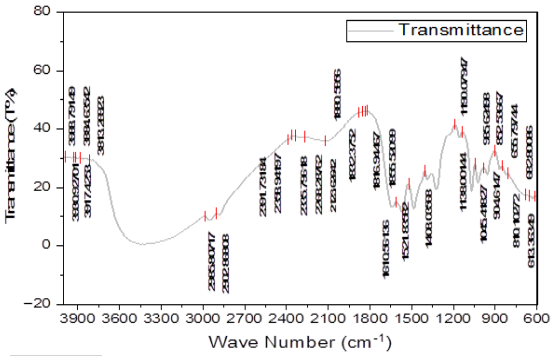

Fig. 24 FTIR Spectra of the Third Sample of [1-CHCL] [6-MEA] After Absorption.

According to the above results, there was no change in the chemical structure of the solution after the absorption process, indicating its high efficiency and thermal and chemical stability.

4.OPTIMIZATION CHOICES

Reaction optimization specifies which parameters best respond. This study used three variables, i.e., concentration, absorption rate, CO_2 loading, and solubility, to determine the maximum CO_2 outflow. The primary purpose of this research is to determine the optimal operating parameters (temperature, concentration, and absorption duration) for maximal absorption. Obtaining the optimal working conditions is shown in Table 5, in which the temperature, solvent concentration, and absorption time for [1-chcl] are 29.025 °C, 1.878 mol/l, and 101.058 min, respectively. These values for [6-MEA] are economically beneficial compared to prior investigations; however, the absorption efficiency decreased under these conditions. The first solvent [1-Chcl] [6-MEA] was better than the monoethanolamine solvent under the best conditions, as it achieved a higher (absorption rate, CO_2 loading, and solubility). Also, the solubility in [1-Chcl] [6-MEA] was higher than monoethanolamine because mixing DESs with aqueous amine reduced the saturated vapor pressure of the substance by adding DESs-

water of 1-choline chloride-6-monoethanolamine; also water losses decreased using an aqueous solution because the carbonate formed by the interaction of MEA with CO_2 was insoluble in monoethanolamine [18]. The CO_2 dissolution behaviors of conventional DESs were unique, e.g., increased carbon dioxide solubility and lower volume expansion, which may be due to the free-size mechanism in which CO_2 molecules occupy vacant holes in DESs previously available within the relatively solid ion structure. Although the HBD structure was less impacted, the HBA structure appeared to be one of the most important in determining the solubility of CO_2 [22].

Table 5 Process Optimization Solution for [1-chcl] [6-MEA].

NO.	Temp.	Conc.	Time	CO_2 Outlet (%)	Absorption Rate (mol/kg.min)	CO_2 Loading (mol/kg)	Absorption Capacity (mg Co_2/g Solvent)	Solubility (mole Co_2/mole)	Desirability
1	29.025	1.878	101.058	2.233	0.0734	7.413	326.189	0.118	Selected
2	35.000	3.000	90.000	10.134	0.0285	2.565	147.724	0.048	
3	45.000	3.000	60.000	3.876	0.0644	2.848	127.882	0.043	
4	35.000	1.500	90.000	4.743	0.0595	5.355	214.357	0.123	
5	45.000	3.000	120.000	14.743	0.00173	0.0208	17.823	0.048	
6	25.000	0.000	60.000	0.6	0.0866	5.196	228.624	0.05	
8	45.000	0.000	60.000	0.545	0.0875	5.253	231.500	0.136	
9	25.000	3.000	120.000	14.955	0.0005	0.0672	2.9568	0.084	
10	25.000	1.500	90.000	10.654	0.0251	2.259	99.497	0.123	

5.MASS TRANSFER COEFFICIENT

The mass transfer coefficient was calculated by dividing the reaction rate by the partial pressure of the best solvent [1-CHCL] [6-MEA] under the best conditions at a temperature of 29°C and concentration of solvent 1.8 mol/l at a time 101 min. The results showed that the value of the mass transfer coefficient equaled (0.145) mol/bar.l.min. Moreover, it was found that the deep eutectic solvent has a higher mass transfer coefficient than the monoethanolamine solvent, which equaled (0.152) mol/ bar.l.min due to the deep eutectic viscosity, which significantly reduced the CO_2 absorption, is one of the most significant challenges [23]. The overall mass transfer coefficient (K_G) can be calculated by the following Eqs. (10) - (12) [24]. The overall mass transfer was calculated according to [15].

$$R_{CO_2}\,â = KG\,.\,P_{CO_2} \quad \textbf{(10)}$$

Where:

KG: Mass transfer coefficient (mol/bar.l².min)

R_{CO_2} â: CO_2 reaction rate (mol/l.min).

P_{CO_2}: Partial pressure of CO_2 (bar).

$$P_{CO_2} = \frac{nRT}{V} = \frac{3\times 10^{-3}\times 0.008314\times 302}{50\times 10^{-3}} = 0.151 \text{ bar} \quad \textbf{(11)}$$

$$R_{CO_2}\,â = KG\,.\,P_{CO_2} \rightarrow KG = \frac{R_{CO_2}\,â}{P_{CO_2}} = \frac{0.023}{0.151} \quad \textbf{(12)}$$

$$KG = 0.152 \ \text{mol/bar.l}^2\,.\,\text{min}$$

6.COMPARISON WITH OTHER STUDIES

It would have been advantageous to investigate the equation established from the statistical investigations, which estimate CO_2 absorption capacity while considering operating circumstances and water content in the present study. Applying this equation, a projection for the CO_2 absorption capacity of pure ChCl-MEA 1:6 DES at (35°C, 1 bar) was produced, obtaining a value of 0.044 mol CO_2/mol DES. This estimate closely matches the previously published value of 0.043 mol CO2/mol DES Islam et al. [25]. Sarmad et al. [26] studied the CO_2 absorption capability of ChCl-MEA 1:6 DES at absorption pressures ranging from 10 to 20 bar in their study. The CO_2 absorption capacity of ChCl-MEA 1:6 DES was determined to be 0.0210 mol CO_2/mol DES at (25 °C, 1 bar). This result is equivalent to the 0.203 mol CO_2/mol DES value reported in the present study. The disparity in results might be attributable to a difference in operating temperatures in the present study, which was done at 45 °C, and Sarmad et al.'s [27] study was conducted at 25 °C. According to Sarmad et al. [26], the minor variation in molar ratios between 1:6 in this research and 1:7 in Sarmad et al.'s study does not result in a substantial change in CO_2 absorption capacity. Sarmad et al. [27] achieved a CO_2 absorption capacity value of 0.290 mol CO_2/mol DES in tests at (25 °C and 20 bar), which is equivalent to the estimated value of 0.301 mol CO_2/mol DES derived using the equation used in this study.

7. CONCLUSIONS

The present study presents novel data about the solubility of CO_2 in amine-based DESs, notably ChCl-MEA, at a molar ratio of 1:6. The results showed that DESs formulated with amines have much better CO_2 absorption capacity than pure amine solvents and typical DESs. It was found that increasing the amine's molar ratio in the DES increased CO_2 solubility. ChCl-MEA had the greatest CO_2 absorption capability among the examined compounds, exceeding monoethanolamine. The increase in CO_2 absorption per mol of ChCl-MEA DES was

observed when the DES had high water content, low temperature, and high pressure. This phenomenon in the DES can be attributed to the improved mass transfer of CO_2 in the presence of water. It was found that the maximum CO_2 absorption capacity reached 0.379 mol CO_2/mol DES when the DES was absorbed with water at 29 °C and 1 bar. The rate of CO_2 absorption by ChCl-MEA DES was influenced positively by pressure and the amount of water present. However, the interaction between these two factors did not result in a synergistic effect, as a water content of up to 50% v aided in the dispersion of the absorbent but did not alter the absorption mechanism. Gas analysis reveals that increasing the absorption pressure allowed a higher intake of CO_2. However, when the temperature rose from 29 °C to 45 °C, the concentration of CO_2 in the air decreased from 85.14 % to 67.13 %, primarily due to increased CO_2 absorption. The solvent concentration negatively impacted the amount of CO_2 absorbed, suggesting that CO_2 absorption by ChCl-MEA DES was more effective at lower temperatures, resulting in an increasing CO_2 absorption capacity and concentration in the output gas. Before DES can be utilized in commercial applications, several challenges must be addressed. These include the high viscosity of DES, the lack of research on amine-based DES regeneration, and toxicity evaluation. Mathematical models, molecular simulations, and process simulations could aid in understanding how DES absorbs CO_2; however, it will take time to reduce the cost of the amine capture process. Thermogravimetric analyses have shown that DES-based products are more thermally stable than freestanding MEA, and the degradation temperature of ChCl-MEA 1:6 was around 140 °C. Deep eutectic amino solvents were useful because they fix broken amines and prevent them from being lost through evaporation.

ABBREVIATION

HBA	Hydrogen Bond Acceptor
HBD	Hydrogen Bond Donor
AMP	2-amino-2-methyl-1-propanol
CCU	Carbon capture and utilization
ChCl	Choline Chloride
DEA	diethanolamine
DES	Deep Eutectic Solution
FITR	Fourier-transform infrared spectroscopy
GHGs	Greenhouse gases
ILs	Ionic liquid solvent
MEA	Monoethnaolamine

REFERENCES

[1] Abdulqadir D, Ibraheem FH. **Utilizing LPG as an Additive to Enhance the Properties of Iraqi Diesel Oil.** *Tikrit Journal of Engineering Sciences* 2023; **30**(2): 10–20.

[2] Jasim DJ, Mohammed TJ, Abid MF, Tahir HH. **Analysis and National Solution for CO2 Gas in Missan Oil Field.** *IOP Conference Series: Earth and Environmental Science* 2021; **779**(1): 12096, (1-9).

[3] Jasim DJ, Mohammed TJ, Harharah HN, Harharah RH, Amari A, Abid MF. **Modeling and Optimal Operating Conditions of Hollow Fiber Membrane for CO2/CH4 Separation.** *Membranes* 2023; **13**(6): 557, (1-29).

[4] Mohammed MN, Yusoh K Bin, Ismael MN, Shariffuddin JHBH. **Synthesis of Thermo-Responsive Poly (N-Vinylcaprolactam): RSM-based Parameters Optimization.** *Multiscale and Multidisciplinary Modeling, Experiments and Design* 2019; **2**: 199–207.

[5] Mohammed MN, Yusoh K Bin, Shariffuddin JHBH. **Parametric Optimization of the Poly (Nvinylcaprolactam) (PNVCL) Thermoresponsive Polymers Synthesis by the Response Surface Methodology and Radial Basis Function Neural Network.** *MATEC Web of Conferences* 2018; **225**: 02023, (1-7).

[6] Jasim MN, Mohammed TJ, Karim AMA. **The Use of Eutectic Solvents for the Enhanced Treatment Carbon Dioxide Gas During the Absorption of Gases Related to the Oil Industries: A Review.** *Iraqi Journal of Oil and Gas Research (IJOGR)* 2022; **2**(2): 60–78.

[7] Uthman OR, Akinola AA, Usman MA, Adepitan A. **Developing a New Empirical-Computational Method, for Accurate Acid-Base Quantitative Analysis.** *Tikrit Journal of Engineering Sciences* 2019; **26**(3): 19–30.

[8] Lu W, Liu S, Wu Z. **Recent Application of Deep Eutectic Solvents as Green Solvent in Dispersive Liquid–Liquid Microextraction of Trace Level Chemical Contaminants in Food and Water.** *Critical Reviews in Analytical Chemistry* 2022; **52**(3): 504–518.

[9] Cao J, Zhang D, Zhang X, Zeng Z, Qin J, Huang Y. **Strategies of Regulating Zn $^{2+}$ Solvation Structures for Dendrite-Free and Side Reaction-Suppressed Zinc-Ion Batteries**. *Energy & Environmental Science* 2022; **15**(2): 499–528.

[10] Hong S, Shen X-J, Xue Z, Sun Z, Yuan T-Q. **Structure – Function Relationships of Deep Eutectic Solvents for Lignin Extraction and Chemical Transformation.** *Green Chemistry* 2020; **22**(21): 7219–7232.

[11] Li Z, Wang L, Li C, Cui Y, Li S, Yang G, et al. **Absorption of Carbon Dioxide Using Ethanolamine-Based Deep Eutectic Solvents.** *ACS Sustainable Chemistry & Engineering* 2019; **7**(12): 10403–10414.

[12] Liu X, Gao B, Jiang Y, Ai N, Deng D. **Solubilities and Thermodynamic Properties of Carbon Dioxide in Guaiacol-Based Deep Eutectic Solvents.** *Journal of Chemical & Engineering Data* 2017; **62**(4): 1448–1455.

[13] Saleh SR, Wiheeb AD. **Kinetic Study of Carbon Dioxide Reaction with Binding Organic Liquids.** *Tikrit Journal of Engineering Sciences* 2019; **26**(1): 26–32.

[14] Lee D, Go W, Oh J, Lee J, Jo I, Kim K-S, et al. **Thermodynamic Inhibition Effects of an Ionic Liquid (Choline Chloride), A Naturally Derived Substance (Urea), and their Mixture (Deep Eutectic Solvent) on CH4 Hydrates.** *Chemical Engineering Journal* 2020; **399**: 125830.

[15] Sayar SS, Mohammed TJ, Karim AMA. **Carbon Dioxide Absorption By 1-Butyl-3-Methyl-Imidazolium Tetraflouroborate [Bmim][BF4].** *Iraqi Journal of Oil & Gas Research* 2022; **2**(2): 1-12.

[16] Nakrak S, Tontiwachwuthikul P, Gao H, Liang Z, Sema T. **Comprehensive Mass Transfer Analysis of CO2 Absorption in High Potential Ternary AMP-PZ-MEA Solvent Using Three-Level Factorial Design.** *Environmental Science and Pollution Research* 2023; **30**(4): 10001–10023.

[17] Abdel-Rahman ZA, Abdullah ZA. **Utilization of CO2 in Flue Gas for Sodium Bicarbonate Production in a Bubble Column.** *Tikrit Journal of Engineering Sciences* 2019; **26**(2): 28–38.

[18] Hsu Y-H, Leron RB, Li M-H. **Solubility of Carbon Dioxide in Aqueous Mixtures of (Reline+ Monoethanolamine) at T= (313.2 to 353.2) K.** *The Journal of Chemical Thermodynamics* 2014; **72**: 94–99.

[19] Lv B, Guo B, Zhou Z, Jing G. **Mechanisms of CO2 Capture Into Monoethanolamine Solution with Different CO2 Loading During the Absorption/Desorption Processes.** *Environmental Science & Technology* 2015; **49**(17): 10728–10735.

[20] Robinson K, McCluskey A, Attalla MI. **An ATR-FTIR Study on the Effect of Molecular Structural Variations on the CO2 Absorption Characteristics of Heterocyclic Amines, Part II.** *ChemPhysChem* 2012; **13**(9): 2331–2341.

[21] Jackson P, Robinson K, Puxty G, Attalla M. **In Situ Fourier Transform-Infrared (FT-IR) Analysis of Carbon Dioxide Absorption and Desorption in Amine Solutions.** *Energy Procedia* 2009; **1**(1): 985–994.

[22] Concepción EI, Moreau A, Vega-Maza D, Paredes X, Martín MC. **Heat Capacities of Different Amine Aqueous Solutions at Pressures Up to 25 MPa for CO2 Capture.** *Journal of Molecular Liquids* 2023; **377**: 121575, (1-12).

[23] Das I, Swami KR, Gardas RL. **Influence of Alkyl Substituent on Thermophysical Properties and CO2 Absorption Studies of Diethylenetriamine-Based Ionic Liquids.** *Journal of Molecular Liquids* 2023; **371**: 121114.

[24] Rashidi H, Valeh-e-Sheyda P, Sahraie S. **A Multiobjective Experimental Based Optimization to the CO2 Capture Process Using Hybrid Solvents of MEA-MeOH and MEA-Water.** *Energy* 2020; **190**: 116430.

[25] Islam SZ, Arifuzzaman M, Rother G, Bocharova V, Sacci RL, Jakowski J, et al. **A Membrane Contactor Enabling Energy-Efficient CO2 Capture from Point Sources with Deep Eutectic Solvents.** *Industrial & Engineering Chemistry Research* 2023; **62**(10): 4455-4465.

[26] Sarmad S, Nikjoo D, Mikkola JP. **Amine Functionalized Deep Eutectic Solvent for CO2 Capture: Measurements and Modeling.** *Journal of Molecular Liquids* 2020; **309**: 113159, (1-43).

[27] Sarmad S, Mikkola J, Ji X. **Carbon Dioxide Capture with Ionic Liquids and Deep Eutectic Solvents: A New Generation of Sorbents.** *ChemSusChem* 2017; **10**(2): 324–352.